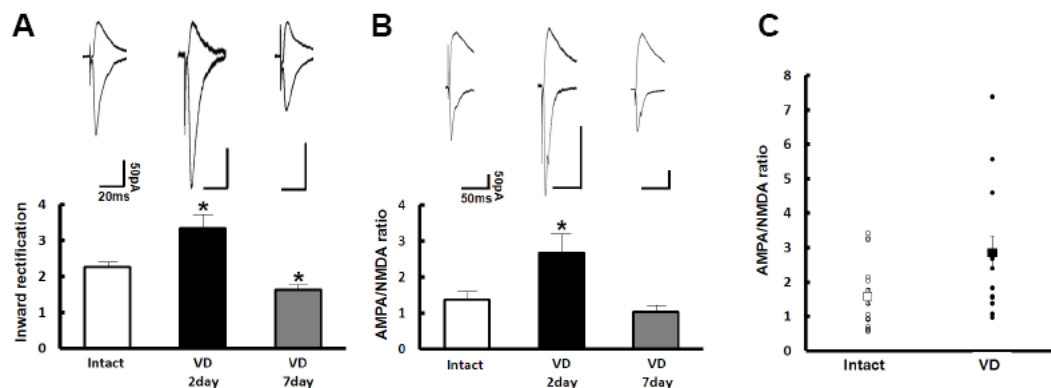


Serotonin Mediates Cross-Modal Reorganization of Cortical Circuits

Susumu Jitsuki, Kiwamu Takemoto, Taisuke Kawasaki, Hirobumi Tada, Aoi Takahashi, Carine Becamel, Akane Sano, Michisuke Yuzaki, R. Suzanne Zukin, Edward B. Ziff, Helmut W. Kessels, and Takuya Takahashi



Jitsuki et al., FigS1

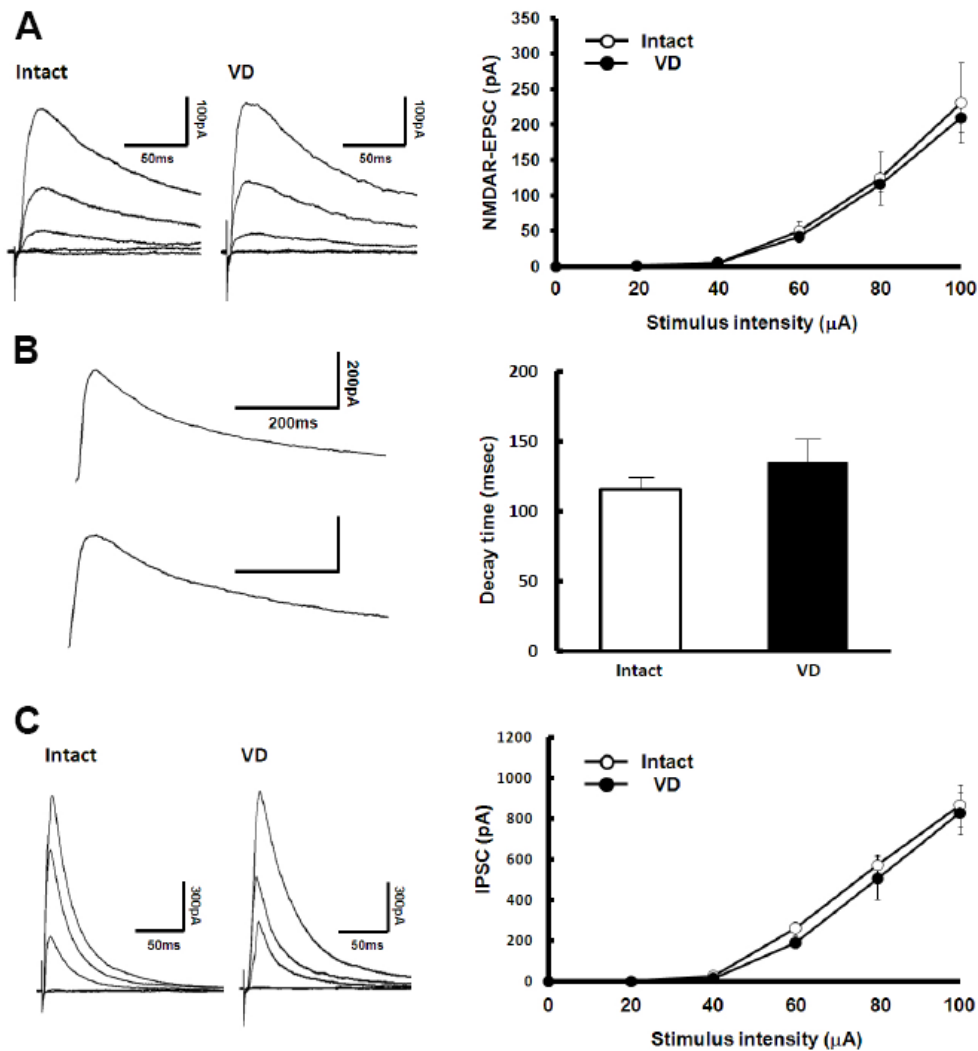
Figure S1 (related to Figure 1)

Behavior of endogenous AMPARs during VD

(A) (Top) Synaptic responses from layer 4 to layer 2/3 pyramidal neurons in the barrel cortex of rats with intact or sutured eyes (VD for 2days and 7days). (Bottom) Graph of average RI of neurons from intact (white) and VD-animals (VD for 2 days and 7days). Note that RI was significantly increased in animals with VD for 2 days (black) but decreased 7 days after VD (gray). Intact animals: n=12, VD for 2 days: n=10, VD for 7 days: 10. Scale bars are as indicated. * shows statistical difference ($p < 0.05$, ANOVA): VD for 2days vs intact, VD for 7 days vs intact. Error bars indicate \pm SEM.

(B) (Top) Synaptic responses from layer 4 to layer 2/3 pyramidal neurons in the barrel cortex of rats with intact or sutured eyes (VD for 2days and 7days). (Bottom) Graph of mean ratio of AMPARs-mediated currents to NMDA receptor-mediated currents (A/N ratio) of VD-rats. Note that A/N ratio of 2 days-VD-rats (black) was larger than that of intact rats (white) and 7 days-VD-animals (gray). Intact: n=8, 2 days-VD: n=13, 7 days-VD: n=9. Scale bars are as indicated. * shows statistical difference ($p < 0.05$, ANOVA): VD for 2days vs intact. Error bars indicate \pm SEM.

(C) A scatter plot (raw data) of A/N ratio of intact and 2-days-VD animals.



Jitsuki et al., FigS2

Figure S2 (related to Figure 2)

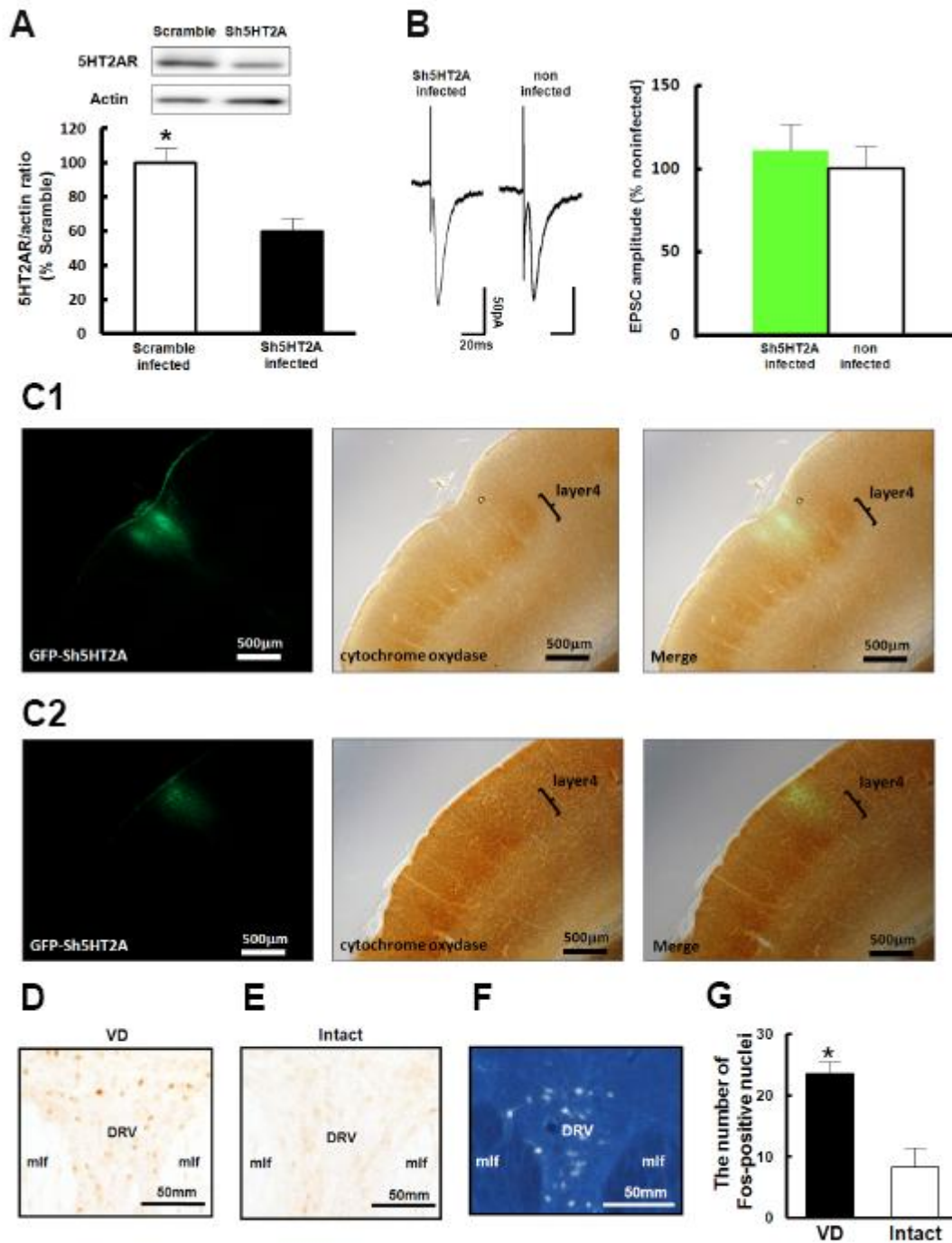
VD did not alter properties of NMDA component and inhibitory component.

(A) (Left) NMDA-receptors mediated synaptic responses from layer 4 to layer 2/3 pyramidal neurons in the barrel cortex of rats with intact or sutured eyes (2days of VD) with different stimulus intensities. (Right) Input-output relations of NMDA currents from intact (open circle) and VD (2 days) animals (black circle). Note that no significant difference was detected between intact and VD-animals. Intact: n=12, VD: n=11. Scale bars are as indicated. Error bars indicate \pm SEM.

(B) (Left) NMDA receptors-mediated synaptic responses from layer 4 to layer 2/3 pyramidal neurons in the barrel cortex of rats with intact or sutured eyes (2 days of VD). No difference in decay kinetics of the NMDA component between intact and VD animals. (Right) Graph of decay kinetics of NMDA component from intact (white) and VD-animals (black). Intact: n=12, VD: n=11. Scale

bars are as indicated. Error bars indicate \pm SEM.

(C) GABA-receptors mediated synaptic responses from layer 4 to layer 2/3 pyramidal neurons in the barrel cortex of rats with intact or sutured eyes (2 days of VD) with different stimulus intensities. (Right) Input-output relations of inhibitory currents from intact (open circle) and VD (2 days) animals (black circle). Note that no significant difference was detected between intact and VD-animals. Intact: n=11, VD: n=10. Scale bars are as indicated. Error bars indicate \pm SEM.



Jitsuki et al., Fig S3

Figure S3 (related to Figure 3)
Serotonin mediates VD-induced AMPARs delivery

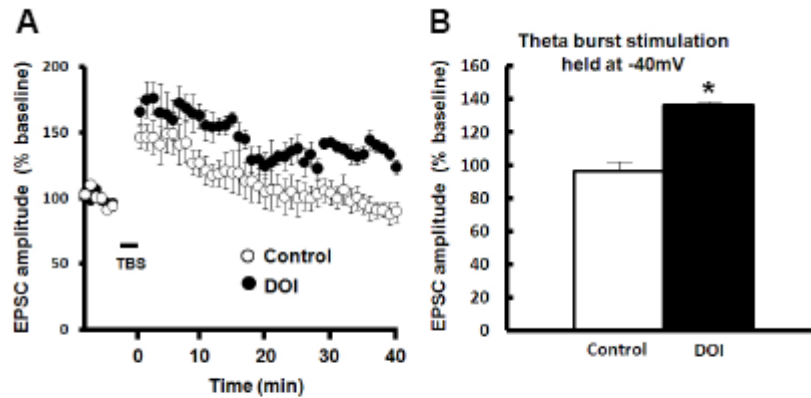
(A) Sh5HT2A reduced the expression of endogenous 5HT2A receptors. Lenti virus expressing either Sh5HT2A or a scramble construct was injected into layer 2/3 of the barrel cortex at P15 *in vivo*. Brain lysate was prepared at P23. The amount of endogenous 5HT2A receptors were assessed with immunoblotting. The amount of actin was used as a reference for the quantitative analysis. n=6. * shows statistical difference ($p < 0.05$, Student's *t*-test). Error bars indicate \pm SEM.

(B) The expression of Sh5HT2A did not alter AMPARs-mediated synaptic transmission in intact animals. (Left) AMPARs-mediated synaptic responses from layer 4 to layer 2/3 pyramidal neurons expressing Sh5HT2A in the barrel cortex of intact rats. Note that there was no significant difference between Sh5HT2A expressing and nearby nonexpressing neurons. n=8. Scale bars are as indicated. Error bars indicate \pm SEM.

(C1,2) Typical examples of tissues expressing GFP-Sh5HT2A. Cytochrome oxydase staining revealed layer4 of the barrel cortex (middle panel). Note that majority of infected area was located in layer2/3. Scale bars are as indicated.

(D-G) VD increases c-Fos expression in the dorsal raphe nucleus.

(D, E) Representative photomicrographs of c-Fos immunoreactive cells in the dorsal raphe nucleus of VD (D) and intact (E) animals. (F) The photomicrographs of fluorogold-positive cells in the dorsal raphe nucleus. Fluorogold was injected into one barrel column of barrel cortex. (G) Graph of average number of Fos-positive nuclei in rats with VD (black) and intact rats (white) in fluorogold positive areas. Note increased number of c-Fos positive neurons in the dorsal raphe of rats with VD than intact rats, indicating that VD rats exhibited higher neuronal activity of serotonergic neurons which project into the barrel cortex. DRV, dorsal raphe nucleus, ventral part; mlf, medial longitudinal fasciculus. n=3. Scale bars are as indicated. * shows statistical difference ($p < 0.05$, Student's *t*-test). Error bars indicate \pm SEM.

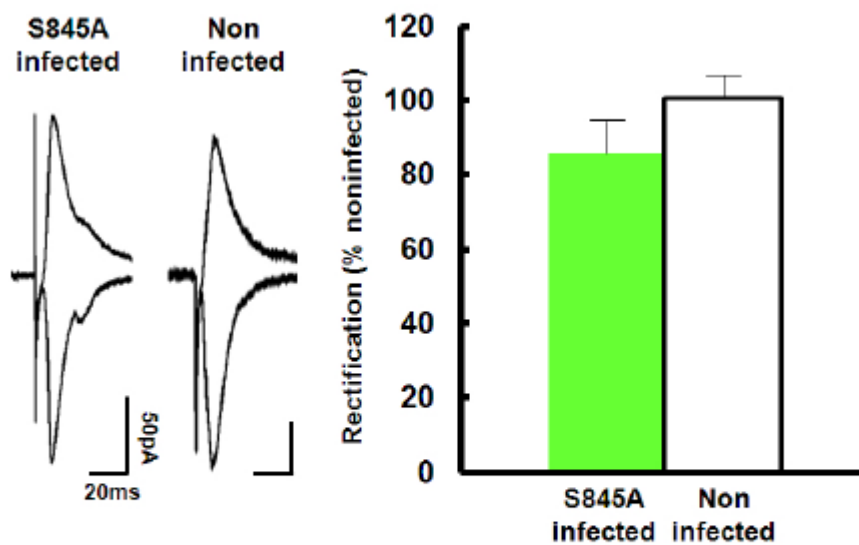


Jitsuki et al., FigS4

Figure S4 (related to Figure 4)

DOI facilitates TBS-induced LTP.

(A) Synaptic plasticity was induced by theta burst stimulation (TBS) with postsynaptic potential at -40 mV with (black) or without DOI (white). The EPSC amplitude was normalized to the average baseline amplitude before pairing. (B) Mean amplitude between 30 min and 40 min after TBS was normalized to base line amplitude. Note that this protocol induced LTP in the presence of DOI (black), while no potentiation was observed in the absence of DOI (white). Control: n=5, DOI: n=4. * shows statistical difference ($p < 0.05$, Student *t*-test). Error bars indicate \pm SEM.



Jitsuki et al., FigS5

Figure S5 (related to Figure 5)

VD did not drive GluR1 S845A mutant into layer 4-2/3 synapses in the barrel cortex.

(Left) Synaptic responses from layer 4 to layer 2/3 pyramidal neurons infected with GFP-GluR1 mutant (S845A) expressing virus and noninfected neurons of VD-rats (2 days). Note no difference of rectification between infected and noninfected neurons. (Right) Graph of average RI of neurons expressing S845A (green), normalized to RI value of nearby noninfected cells (white). n=7. Scale bars are as indicated. Note that there was no statistical difference. Error bars indicate \pm SEM.

Supplemental Experimental Procedures

Constructs

Constructs of AMPA receptor subunits tagged with GFP (GFP-GluR1, GFP-GluR1ct) and Herpes viruses were prepared as previously described (Shi et al., 2001). The S845A mutation on GluR1 was introduced into GFP-GluR1 using the overlap extension polymerase chain reaction (PCR). The PCR fragments were sub-cloned into the pHSVPrPUC vector using HindIII and XbaI. The shRNA targeting 5-HT2A receptor mRNA from rat, mouse and human (tgctgttgacagtgagcgacGTAGGTATATCCATGCCAAttagtgaagccacagatgtaaTTGGCATGGATATA CCTACggtgectactgctcgga) was amplified by PCR and first sub-cloned into the pENTR expression vector using the XhoI and EcoR1 enzymes and then subcloned into the pFUGW vector (Lois et al.,

2002). The control shRNA (Scr) targeted GGTAAGTGCCCAAATATCT, a sequence not present in known rat, mouse and human genes or ESTs. ShRNA-resistant 5HT2AR (res-5HT2AR) construct was generated by mutating the 5HT2AR-ShRNA target at five different nucleotides without changing the amino acid sequence. Mutations were introduced using the QuickChange mutagenesis. For lentiviral expression, constructs were subcloned into CSII-EF-MCS-IRES2-hKO1 vector (kindly provided by Dr. Hiroyuki Miyoshi, RIKEN, Tsukuba, Japan) using EcoR1 and Not1. All constructs were confirmed by DNA sequencing.

Electrophysiology

36 hour after virus injection, rats were anesthetized with isoflurane gas and brains were removed. Brains were quickly transferred into ice-cold dissection buffer (25.0mM NaHCO₃, 1.25mM NaH₂PO₄, 2.5mM KCl, 0.5mM CaCl₂, 7.0mM MgCl₂, 25.0mM glucose, 110.0mM choline chloride, 11.6mM ascorbic acid, 3.1mM pyruvic acid) gassed with 5% CO₂/95% O₂. Coronal brain slices were cut (300 μm, Leica vibratome) in dissection buffer and transferred to physiological solution (22-25°C, 118mM NaCl, 2.5mM KCl, 26.2mM NaHCO₃, 1mM NaH₂PO₄, 11mM glucose, 1.3mM MgCl₂, 2.5mM CaCl₂, Ph7.4, gassed with 5% CO₂/95% O₂). The recording chamber was perfused with physiological solution containing 0.1mM picrotoxin, 4μM 2-chloroadenosine at 22-25°C For rectification experiments, we added 0.1mM D,L-APV to perfusate to block NMDARs. Patch recording pipettes (3-7 MΩ) were filled with intracellular solution (115mM cesium methanesulfonate, 20mM CsCl, 10mM HEPES, 2.5mM MgCl₂, 4mM Na₂ATP, 0.4mM Na₃GTP, 10mM sodium phosphocreatine, 0.6mM EGTA at PH7.25). Whole-cell recordings were obtained from infected or uninfected layer 2/3 pyramidal neurons (150 - 500 μm from pial surface) of the rat barrel cortex with Multiclamp 700B (Axon Instruments). There were no significant differences in input or series resistance among groups (infected, non-infected, intact, deprived). Bipolar tungsten stimulating electrodes were placed in layer 4 ~200-300μm below recorded cells. Stimulus intensity was increased until a synaptic response of amplitude > ~10 pA was recorded. When recording simultaneously from two cells, stimulus intensity was increased until a) both cells showed response > ~10 pA, or b) one cell showed response > ~10 pA and a stronger stimulus produced epileptiform bursting. Synaptic AMPA-R mediated responses at -60mV and +40mV were averaged over 50-100 trials and their ratio was used as an index of rectification (Shi et al., 2001). For paired recordings, infected and nearby uninfected cells (~50μm) were whole-cell accessed and a synaptic response to stimulus was recorded from both cells simultaneously. AMPA/NMDA ratios were calculated as the ratio of peak current at -60mV to the current at +40mV 50ms after stimulus onset (40-50 traces averaged for each holding potential). For analyzing inward rectification (recorded from noninfected animals: Figure 1H, S1A), intracellular solution containing 0.2mM spermine (115mM cesium methanesulfonate, 20mM CsCl, 10mM HEPES, 2.5mM MgCl₂, 4mM Na₂ATP, 0.4mM Na₃GTP,

10mM sodium phosphocreatine, 0.6mM EGTA at PH7.25) was used. Inward Rectification was calculated by dividing the absolute amplitude of average EPSC measured at -60 mV by that at $+40$ mV.

In experiments analyzing long-term potentiation in slices from visually deprived or intact rats were maintained in ACSF. In a subset of experiments standard ACSF was used as described above. In order to monitor synaptic transmission we evoked AMPA post synaptic currents at two synaptic pathways by interleaved stimulation of two fiber bundles at 0.33 to 0.1Hz and recorded at -60 mV holding potential in voltage-clamp mode. LTP was induced at one pathway by a pairing protocol consisting of presynaptic fiber stimulation at 5Hz for 90 sec paired with postsynaptic depolarization to 20 mV holding potential in occlusion experiments. For experiments to examine the effect of DOI on LTP, we paired 1 Hz stimulation (3 min) with postsynaptic potential either at -40 mV or 0mV. For theta burst stimulation (TBS), layer4-2/3 synapses were stimulated with 5 Hz trains of 5 theta bursts containing five pulses at 100 Hz (bursts were separated by 200 ms). The postsynaptic potential was held at -40 mV, when TBS was applied and switched back to -60 mV afterward. Experiments were excluded from analysis if unpaired control pathways displayed changes in transmission.

To record input-output relations of layer 4-2/3 synapses, stimulating electrodes were placed in layer 4 200 μ m below recorded cells. NMDA receptor-mediated EPSCs were recorded at $+40$ mV perfused with ACSF containing 0.1mM picrotoxin, 4 μ M 2-chloroadenosine, and IPSCs were recorded at 0mV perfused with ACSF containing 0.1mM D,L-APV, 4 μ M 2-chloroadenosine. Input-output curves were generated by systematically adjusting the stimulation intensity from 20 to 100 μ A.

For the recording of the asynchronous quantal AMPAR-EPSCs (Sr^{2+} -mEPSCs), CaCl_2 was replaced with 2mM SrCl_2 , and 2-chloroadenosine was removed. Sr^{2+} -mEPSCs were detected and analyzed using Clampfit10.2 software (Axon Instruments). The detection threshold for Sr^{2+} -mEPSCs was set at 10 pA (2X RMS noise). Asynchronous synaptic events were picked up from events that occurred between 200 and 900msec after the stimulation.

Infection of neocortical neurons in vivo

At PND21, rats were anesthetized with a ketamine/xylazine cocktail (ketamine: 0.56mg/g body weight; xylazine: 0.03mg/g body weight). The skin overlying the skull was cut and gently pushed to the side. The anterior fontanel was identified and a region 2mm posterior, 5 mm lateral was gently pierced with a dental drill. Coordinates were independently ascertained to correspond to the barrel cortex by cytochrome oxidase staining. Glass pipettes (tip diameter $\sim 12\mu$ m) were used to inject recombinant Herpes virus into the barrel cortex. After injection, the skin was repositioned and maintained with cyanoacrylate glue. During procedures, animals were kept on a heating pad and

were brought back into their home cages after regaining movement. Visual deprivation was initiated by suturing eyelids immediately after injection of virus.

For biochemical analysis, A craniotomy (2mm x 2mm) was opened above the barrel cortex was opened above barrel cortex centered on bregma 2 mm and lateral 5mm. The nine injections were performed at equally-spaced intervals (per hemisphere).

***In vivo* microdialysis**

Visually deprived or intact rats were anesthetized and stereotaxically implanted with stainless-steel guide cannula (outer diameter, 0.51 mm; AG-4, Eicom Co., Kyoto, Japan) into the barrel cortex. The coordinates were 2 mm anterior from the bregma, 4.5 mm lateral to the midline, and 0.2 mm below the surface of the brain. After cannula implantation, a stylet was inserted into the guide until the microdialysis experiment.

Two hour before microdialysis experiment, the stylet was replaced with a dialysis probe with a 1.0-mm-long semipermeable membrane (o.d., 0.31 mm, AI-4-1, Eicom Co.). A two-channel fluid swivel device (SSU-20, Eicom Co.) was connected to the inlet and outlet of the probe and artificial cerebrospinal fluid (147 mM NaCl; 4 mM KCl; 1.2 mM CaCl₂; 0.9 mM MgCl₂) was infused through the probe at a rate of 1.2 µl/min using a microdialysis pump (CMA/102, Carnegie Medicin, Stockholm, Sweden). Each rat was maintained individually in its cage and the dialysis was performed under unanesthetized, unrestrained conditions. Following an overnight equilibrium period, Six samples (36 µl each) were collected every 30 min along 3 hours in vials containing an equal volume (36 µl) of acetic acid solution (40 mM) with EDTA (200 µM). Samples were stored at -70°C until the assay.

5HT assay

5HT concentration in the dialysate was quantified by high performance liquid chromatography with a pump system (EP-300; Eicom Co.). Each 72 µl sample (36 µl of dialysate plus 36 µl of acetic acid solution) was injected into a pre-column (AC-ODS, Eicom Co.) with a mobile phase consisting of 0.1 M phosphate buffer at pH 6.0, 0.13 mM EDTA, 2.3 mM sodium-1-octanesulfonate, and 20% methanol. The 5HT was then separated out with a separation column (CA5-ODS, Eicom Co.) maintained at 25°C and detected with an electrochemical detector (ECD-300, Eicom Co.). The electrode potential was set to 400 mV against an Ag/AgCl reference electrode. The changes in electric current (nA) were recorded using an integrated data processor (Chromatocorder 12; System Instruments Co., Tokyo, Japan). The 5HT concentration in the dialysate was calculated by reference to the peak area of the standard solution.

Biochemical analysis

Barrel cortex samples were rapidly dissected out and stored at -80°C until assayed. Frozen samples were ice-cold homogenation buffer using glass-glass tissue homogenizer. Homogenates were sonicated in 1% SDS and boiled for 10 min. Small aliquots of the homogenate were retained for protein determination by the bicinchoninic acid protein assay method. Equal amounts of protein were processed by using 10% acrylamide gels, and transferred PVDF membranes. Membranes were blocked with either 1% BSA or 4% non-fat dry milk in TBS-TritonX (0.1%) for 1 hour and incubated in primary antibody against p-Ser845 1:1000 (Millipore), GluR1 1:1000 (Millipore), p-ERK 1:500 (Promega), ERK 1:2000 (Upstate), 5HT2AR 1:500 (kindly provided by Dr. Philippe Marin, Institut de génomique fonctionnelle, France), actin 1:6000 (Sigma). Blots were then washed in TBS-TritonX and placed in HRP-conjugated anti-rabbit secondary antibody at 1:1000 dilutions. Blots were then washed and reacted with ECL or ECL-plus reagents. ECL-treated blots were quantified by densitometry using LAS3000 (Fujifilm). The level of the phosphorylated form of a protein was normalized to the total level of the same protein. Data on protein phosphorylation are expressed as percentages of control.

Immunohistochemistry

VD or intact animals were anesthetized with an overdose of sodium pentobarbital, and then perfused transcardially with heparinized saline followed by 4% paraformaldehyde in 0.1 M phosphate buffer (pH 7.4). The brains were removed immediately after perfusion and postfixed in a fixative and saturated in 30% sucrose overnight at 4°C . Coronal sections of the midbrain ($30\ \mu\text{m}$) were prepared with a cryostat. Free-floating sections were preincubated for 2 h with 0.1 M phosphate buffered saline (PBS) containing 2% normal goat serum and 0.1% Triton X-100. After rinsing twice with 0.1 M PBS, sections were incubated overnight at room temperature in a PBS solution containing anti c-Fos polyclonal antibody (1:40000, Calbiochem, USA), 1% normal goat serum and 0.1% Triton X-100. After rinsing twice with 0.1 M PBS, the sections were incubated in 0.1 M PBS containing biotinylated anti-rabbit IgG (1:200, Vector Lab USA) for 1h and then incubated in 0.1 M PBS containing avidin-biotin-peroxidase complex (1:200, Vector Lab, USA) for 1 h at room temperature to amplify the antibody signal. The sections were rinsed with 0.1M phosphate buffer and incubated with 0.05% diaminobenzidine and 0.03% hydrogen peroxide for 5 min at room temperature. The sections were then dehydrated with ethanol and coverslipped. The c-Fos-stained nuclei in the dorsal raphe were counted blindly. Averages from four slices (corresponding to plates 49 in Paxinos and Watson [1997]) per animal were used for statistical analysis.

For fluorogold tracing, rats were anesthetized with a ketamine/xylazine cocktail and injected with 5% fluorogold (Biotium) into the barrel cortex as the same coordination as virus

injection. Two days after injection, rats were sacrificed and brains were fixed as described above. Coronal sections of the midbrain (50 μ m) were prepared with a freezing microtome. Photomicrographs of fluorogold tracing were taken with an epifluorescent microscope providing ultraviolet excitation.

Statistical Methods

Kolmogorov-Smirnov test was used for the analysis of evoked quantal EPSCs (Figure 1G). Wilcoxon nonparametric test was used for the analysis of simultaneous paired recordings (Figure 1C, Figure 3E). Student *t*-test was used for all other experiments.

Supplemental References

Lois, C., Hong, E.J., Pease, S., Brown, E.J., and Baltimore, D. (2002). Germline transmission and tissue-specific expression of transgenes delivered by lentiviral vectors. *Science* 295, 868-872.

Shi, S., Hayashi, Y., Esteban, J.A., and Malinow, R. (2001). Subunit-specific rules governing AMPA receptor trafficking to synapses in hippocampal pyramidal neurons. *Cell* 105, 331-343.